Mechanics & Industry **23**, 8 (2022)

https://doi.org/10.1051/meca/2022007

Mechanics & Industry

Available online at:
www.mechanics-industry.org

REGULAR ARTICLE

OPEN ACCESS

Simulation on the effect of cylinder liner and piston ring surface roughness on friction performance

Na Liu[1,*], Chengnuo Wang[1], Qun Xia[2], Yuanyuan Gao[1], and Peng Liu[1]

[1] College of Mechanical and Electrical Engineering, Shandong Jianzhu University, Jinan Shandong 250101, PR China
[2] Xintai Science and Technology Bureau, Taian Shandong 271200, PR China

Received: 5 November 2021 / Accepted: 4 March 2022

Abstract. Considering the surface roughness of piston ring and cylinder liner and deformation of cylinder liner, the friction dynamics calculation model of cylinder liner-piston ring friction pair was established. The effects of top ring, other piston rings and cylinder liner surface roughness on friction performance were analyzed by grouping comparison and Box-Behnken response surface methodology. The calculation results show that when the surface roughness of the piston ring increases, the friction of the asperity increases slightly, the friction of the fluid decreases, and the total friction loss decreases. When the surface roughness of the cylinder liner increases, the friction of the asperity decreases slightly, the friction of the fluid increases, and the total friction loss increases.

Keywords: Piston ring / cylinder liner / surface roughness / response surface analysis / friction performance

1 Introduction

The cylinder liner-piston ring friction pair mainly plays a sealing role in the internal work of the engine, and the friction loss generated in the work accounts for approximately 26% of the total loss of the engine [1]. It can be seen from previous studies that the operating conditions of the engine [2], the structural parameters of the piston ring and the cylinder liner [3], and the elastic force of the piston ring [4] have different effects on the friction performance of the cylinder liner piston ring friction pair. Since the piston ring and cylinder liner cannot obtain a completely smooth surface in the processing and production process, the micro-convex on the surface also has a certain impact on the friction performance of the friction pair with the cylinder liner piston ring. In addition, adding surface texture on the surface of the piston ring or cylinder liner is also one of the important means to improve friction performance. In recent years, researchers have also conducted in-depth research in the fields of surface roughness and surface texture [5]. For example, Li [6] used AVL -PR to establish the dynamic simulation model of the piston ring group and analyzed the influence of different surface roughness texture directions on the friction performance under different working conditions. The results showed that different surface roughness texture directions had significant indigenous effects on the sealing performance and friction performance of the diesel engine. When the piston ring surface was horizontally textured and the cylinder liner was vertically textured, the sealing performance and friction performance of the engine could be improved. Wu [7] studied the influence of the inner surface mesh of cylinder liner on the friction performance by solving the average Reynolds equation, and found that the a larger roughness or cross-type inner mesh was beneficial for improving the friction performance and reducing the friction loss. Rao [8] analyzed the friction performance of three cylinder liners with different surface textures through wear experiments. The results show that the surface texture shape has an impact on the friction performance, and the surface texture area also has a certain impact on the friction performance. In addition, Liu [9] found that each piston ring in the piston ring group would have mixed lubrication in the work, that is, all piston rings would produce micro-convex friction in the movement, indicating that it is also necessary to study the influence of the structure of different piston rings on the friction performance.

In previous studies, the influence of a single piston ring on the friction performance of cylinder liner piston ring friction pair was mostly studied, but the overall study of the piston ring group was relatively rare. In this paper, taking a single-cylinder diesel engine as the research object, considering the deformation of the engine cylinder liner, surface roughness, and mixed lubrication, a simulation

* e-mail: liuna_sd@sdjzu.edu.cn

model of the cylinder liner-piston ring group is established. In addition to analyzing the influence of surface roughness of top ring and cylinder liner on friction force and friction loss of cylinder liner piston ring friction pair, considering the coupling effect of multiple piston rings, the influence of surface roughness of four piston rings in piston ring group on friction loss was analyzed by response surface methodology. It provides a reference for the optimization design of surface processing of piston ring and cylinder liner of diesel engine.

2 Theoretical basis

2.1 Mean reynolds equation

Considering the effect of roughness on friction performance, the pressure flow factor and shear flow factor are introduced, and the average Reynolds equation proposed by PATIR and CHENG [10] is used to calculate the oil film pressure distribution between the cylinder liner and piston ring.

$$\frac{\partial}{\partial x}\left(\phi_x \rho \frac{h^3}{\mu}\frac{\partial p}{\partial x}\right) + \frac{\partial}{\partial y}\left(\phi_y \rho \frac{h^3}{\mu}\frac{\partial p}{\partial y}\right) = 6U\frac{\partial(\rho\overline{h_t})}{\partial x} + 6U\sigma\frac{\partial(\rho\phi_s)}{\partial x} + 12\frac{\partial(\rho\overline{h_t})}{\partial t}. \quad (1)$$

Therein: ϕ_x, ϕ_y are the axial and circumferential pressure flow factors respectively; ϕ_s is the shear flow factor; ρ is the lubricant density; p is the oil film pressure; U is the movement speed of the piston ring; α is the comprehensive roughness of the two surfaces of the piston ring and the cylinder liner, $\sigma = \sqrt{\sigma_1^2 + \sigma_2^2}$; σ_1 is the surface roughness of the piston ring; α_2 is the surface roughness of the cylinder liner; h is the nominal oil film thickness, $\overline{h_t}$ is the expected value of the actual oil film thickness; μ is the lubricant dynamic viscosity.

Regarding the solution method of the Reynolds equation [11], the finite difference method proposed by SOUTHWELL is one of the earliest classes of solution methods, and it is currently widely used in related research.

The Reynolds equation is solved by determining the boundary conditions, which are the axial boundary conditions of the upper and lower edges of the piston ring and the piston ring opening gap boundary conditions.

Axial boundary conditions:

$$p\left(\frac{b}{2}, y\right) = p_1 \quad (2)$$

$$p\left(-\frac{b}{2}, y\right) = p_2. \quad (3)$$

Therein: p_1 is the gas pressure at the upper edge of the piston ring; p_2 is the gas pressure at the lower edge of the piston ring; b is the axial height of the piston ring.

Opening gap boundary conditions:

$$p(x,0) = p(x,L) = \frac{p_1 - p_2}{b}x + \frac{p_1 - p_2}{2}. \quad (4)$$

Therein: L is the length of the piston ring in the circumferential direction.

2.2 Rough contact model

Due to the roughness between the two surfaces of the piston ring and cylinder liner, when the film thickness ratio $H < 3$ ($H = h/\alpha$), the friction pair is in a mixed lubrication state, and the two surfaces will have micro-convex contact during the relative motion, generating micro-convex contact force. This paper adopts the rough surface contact model proposed by Greenwood and Tripp [12] to calculate the micro-convex contact force between cylinder liner and piston ring [13].

$$W_A = \frac{16\sqrt{2}}{15}\pi(\eta\beta\sigma)E\sqrt{\frac{\sigma}{\beta}}AF_{5/2}(H) \quad (5)$$

$$A_c = \pi^2(\eta\beta\sigma)^2 AF_2(H) \quad (6)$$

$$E = \frac{1}{\left(\frac{1-\nu_1^2}{E_1}\right) + \left(\frac{1-\nu_2^2}{E_2}\right)}. \quad (7)$$

Therein: W_A is the micro-convex contact force; η is the micro-convex density; β is the micro-convex radius of curvature; H is the film thickness ratio; A is the nominal contact surface contact of the micro-convex; A_c is the actual contact area of the micro-convex; E is the integrated elastic modulus of the two surfaces of the piston ring and the cylinder liner; E_1, E_2 are the modulus of elasticity of cylinder liner and piston ring; v_1, v_2 are the Poisson's ratio of cylinder liner and piston ring.

The calculation formulas of $F_{2.5}(H)$ and $F_2(H)$ are as follows:

$$\mathrm{F_{2.5}(H)} = \begin{cases} 0 & \mathrm{H} > 4 \\ 1.12 \times 10^{-4}(4-\mathrm{H})^{1.9447} & 4 \geq \mathrm{H} > 3.5 \\ 2.134 \times 10^{4}\exp\left\{\begin{array}{l} 3.8045\ln(4-\mathrm{H}) \\ +1.34[\ln(4-\mathrm{H}]^2 \end{array}\right\} & \mathrm{H} \leq 3.5 \end{cases} \quad (8)$$

$$\mathrm{F_2(H)} = \begin{cases} 0 & \mathrm{H} > 4 \\ 8.8123 \times 10^{-4}(4-\mathrm{H})^{2.1523} & 4 \geq \mathrm{H} > 3.5 \\ 1.705 \times 10^{-4}\exp\left\{\begin{array}{l} 4.504\ln(4-\mathrm{H}) \\ +1.37025[\ln(4-\mathrm{H}]^2 \end{array}\right\} & \mathrm{H} \leq 3.5. \end{cases} \quad (9)$$

2.3 Piston ring force model

In addition to gravity, the piston ring is mainly subjected to the force of the combustion chamber gas, the piston ring groove, as well as friction and its own elastic force. Figure 1 shows the force diagram when the piston moves upward.

2.3.1 Radial force balance of piston ring

The radial force equilibrium condition of the piston ring in operation is:

$$W_A + F_L = F_g + F_e. \tag{10}$$

Therein: W_A is the micro-convex contact force; F_L is the lubricant fluid force between the cylinder liner piston ring; F_g is the piston ring backlash gas force; F_e is the piston ring's own elastic force.

The lubricant fluid force between the piston ring and the cylinder liner can be obtained by integrating the oil film pressure on the piston ring. The specific calculation formula is:

$$F_L = \iint \mathrm{pdxdy}. \tag{11}$$

The calculation formula of piston ring backlash gas force is:

$$F_g = 9p_g\pi(D - 2T)b. \tag{12}$$

Therein: p_g is the gas pressure of piston ring backlash; D is the diameter of the piston ring; T is the radial thickness of the piston ring; b is the axial height of the piston ring.

The calculation formula of the elastic force of the piston ring is:

$$F_e = \frac{4E_2\frac{S}{T}}{9\left(\frac{D-2T}{T}\left(\frac{D-2T}{T}-1\right)\right)}Db. \tag{13}$$

Therein: E_2 it is the elastic modulus of the piston ring; S is the opening gap of the piston ring.

2.3.2 Piston ring axial force balance

The axial force equilibrium condition of the piston ring in operation is:

$$\mathrm{Mg} + F_2 = F_H + F_A + R_x + F_1. \tag{14}$$

Therein: Mg is the piston ring gravity; F_2 is the gas pressure on the upper surface of the piston ring; F_H is the fluid friction; F_A is the asperity friction; R_x is the support force of the piston ring groove on the lower surface of the piston ring; F_1 is the gas pressure on the lower surface of the piston ring.

The calculation formula of asperity friction and fluid friction is as follows:

$$F_A = \tau_0 A_c + \alpha W_A \tag{15}$$

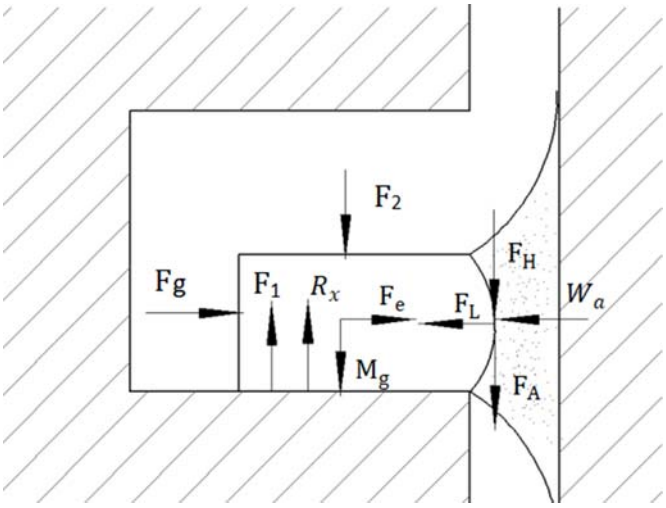

Fig. 1. Piston ring force diagram.

$$F_H = \int_{x_1}^{x_2}(\tau_1 + \tau_2)dx. \tag{16}$$

Therein: τ_0 is the shear stress constant, the value is $2\ X\ 10^6$; α is the boundary friction coefficient; x_1,x_2 are the starting point and ending point of the oil film; τ_1, τ_2 is the shear factor.

2.3.3 Total piston ring friction

The total friction force on the piston ring is mainly composed of lubricant fluid friction and asperity friction between the contact surface of the piston ring and the cylinder liner.

$$F_f = F_H + F_A. \tag{17}$$

Therein: F_f is the total friction force; F_H is the fluid friction force; and F_A is the asperity friction force.

3 Model building

3.1 Engine dynamics model

Taking a single-cylinder diesel engine as the research object, according to the main parameters of the engine in Table 1, the dynamic model of the piston ring friction pair of the cylinder liner is established in AVL EXCITE P&R. The dynamic model mainly consists of piston, cylinder liner, piston ring set, piston pin, connecting rod and other major components, as shown in Figure 2. Figure 3 gives the relative position of the piston and piston ring of the engine. Table 2 presents the mass and basic dimensions of each piston ring.

3.2 Engine thermodynamic model

In addition to the main structural parameters, it is necessary to obtain important parameters such as combustion chamber pressure, temperature, heat transfer coefficient and cylinder liner surface profile during engine operation when building the model.

Table 1. Main engine parameters.

Parameters	Parameter Value
Number of cylinders	1
Stroke	4
Calibration speed	2000 r/min
Bore x stroke	95 mm x 115 mm
Connecting rod length	210 mm
Crankshaft radius	57.5 mm
Compression ratio	20
Lubricants Type	5W-30

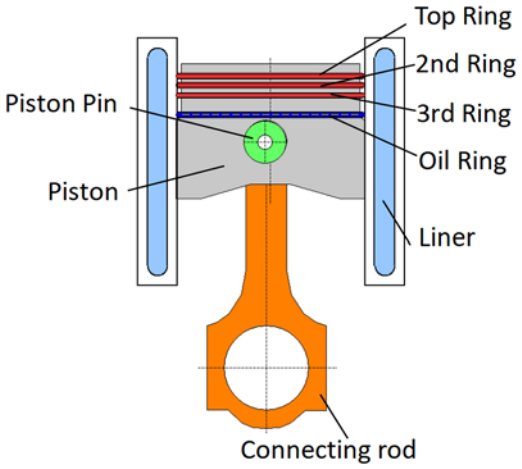

Fig. 2. Dynamics model.

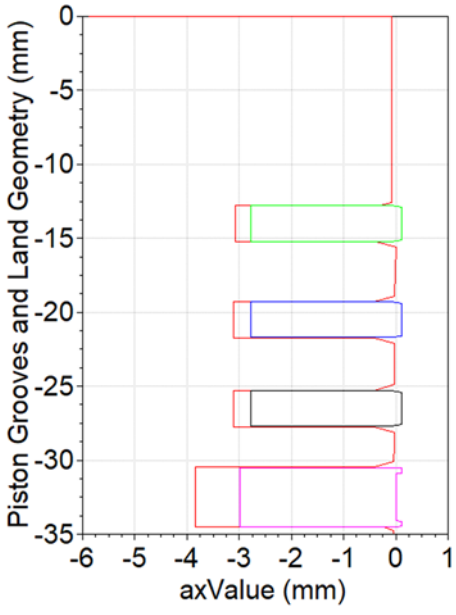

Fig. 3. Relative position of piston ring and piston.

GT-Power is used to establish the thermodynamic model of the engine as shown in Figure 4. Calculation of the thermodynamic parameters of the engine under rated conditions (8.8 kw, 2000 r/min). The change curves of the combustion chamber pressure, temperature and heat transfer coefficient with the crankshaft rotation angle of the engine are calculated in Figures 5, 6 and 7. Based on the data in the figure, the average combustion temperature and the average heat transfer coefficient were obtained as 598 °C and 375 W/m^2 °C, respectively.

The calculated data were compared with the experimental data in previous studies. In [14], combustion pressure reaches a maximum value of approximately 7.6 MPa at 7 °C after the upper dead center of the work stroke, while the cylinder temperature reaches a maximum value of approximately 1980 at 40 °C after the upper dead center. The maximum combustion pressure calculated by this model was 7.5 MPa at 14 °C after the upper dead center, and the maximum combustion temperature was 1939 °C at 34 °C after the upper dead center, indicating that the calculation results of this model were accurate.

3.3 Cylinder liner deformation

During the engine operation, the cylinder liner is slightly deformed by the combustion chamber temperature and other factors for a long time, and its surface profile changes have some influence on the friction performance of the cylinder liner piston ring friction pair [15].

The deformation of the cylinder liner during operation is analyzed by finite element software considering the thermal load of the cylinder liner and its assembly preload. According to the formula given in [16] and the average combustion temperature and heat transfer coefficient of the combustion chamber obtained in Section 3.2, the distribution characteristics of the surface combustion temperature and heat transfer coefficient of the cylinder liner along the axial direction are calculated as:

$$T(s) = T_m \cdot (1 + k_2\gamma) \cdot e^{-\sqrt{\beta}} \tag{18}$$

$$\alpha(s) = \alpha_m \cdot (1 + k_1\gamma) \cdot e^{-\sqrt[3]{\beta}}. \tag{19}$$

Therein: $T(s)$, $\alpha(s)$ are the cylinder liner surface combustion temperature and heat transfer coefficient along with the axial height change; T_m, α_m are the average combustion temperature in the combustion chamber and the heat transfer coefficient; k_1, k_2 are constants, $k_1 = 0.537\,(\mathrm{l/d})^{0.24}$, $k_2 = 1.45k_1$; l is the piston stroke; d is the cylinder liner inner diameter; $\gamma = s/l\,(0 \leq \gamma \leq 1)$, s is the piston axial displacement, $s = 0$ when the piston is located in the upper stop.

The surface combustion temperature and heat transfer coefficient distribution are calculated, which are used as boundary conditions. The temperature field distribution of the cylinder liner is simulated by finite element software,

Table 2. Piston ring mass and dimensional parameters.

	Mass (g)	Ring height (mm)	Ring thickness (mm)
Top ring	21	2.97	3.50
Second Ring	22	3.00	3.56
Three rings	22	3.00	3.56
Oil ring	30	5.58	3.44

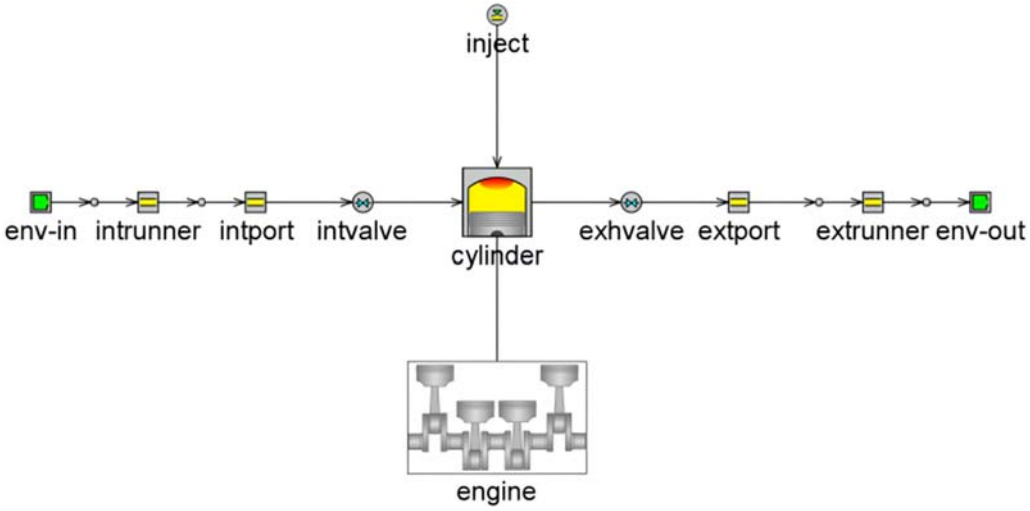

Fig. 4. Engine thermodynamic model.

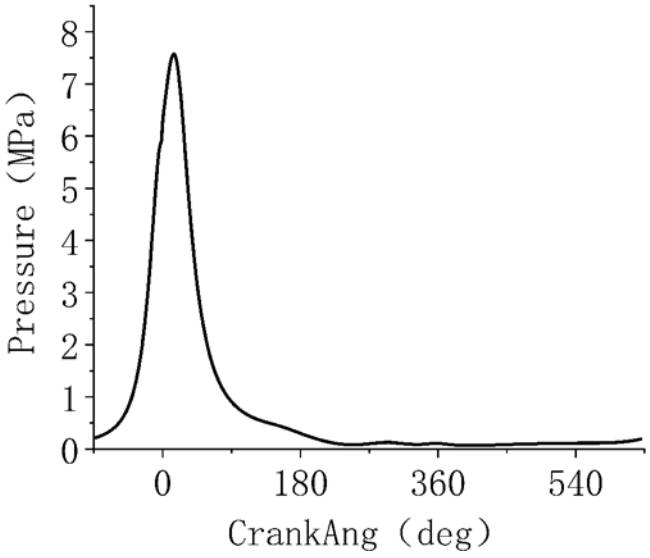

Fig. 5. Combustion chamber pressure variation curve with crankshaft rotation angle.

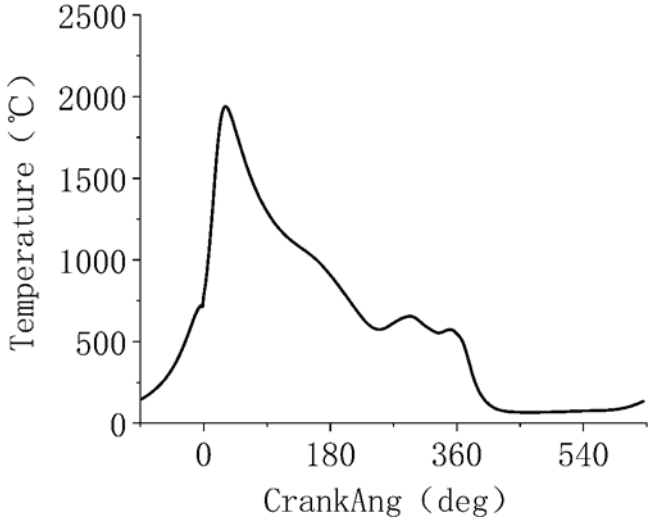

Fig. 6. Combustion chamber temperature variation curve with crankshaft rotation angle.

and the experimental results are compared. Multiple temperature characteristic points are taken in the upper, middle and lower parts of the cylinder liner. The specific temperature measurement points are shown in Figure 8, and the average temperature measurement points in the same plane are calculated. The calculation results are shown in Table 3 with the experimental results [17]. The comparison shows that the temperature numerical error of the corresponding characteristic points is within 3%, indicating that the calculation results of the model are reliable.

After completing the calculation of the deformation of the cylinder liner, 36 paths are taken on the inner surface of the cylinder liner, the radial deformation information of all

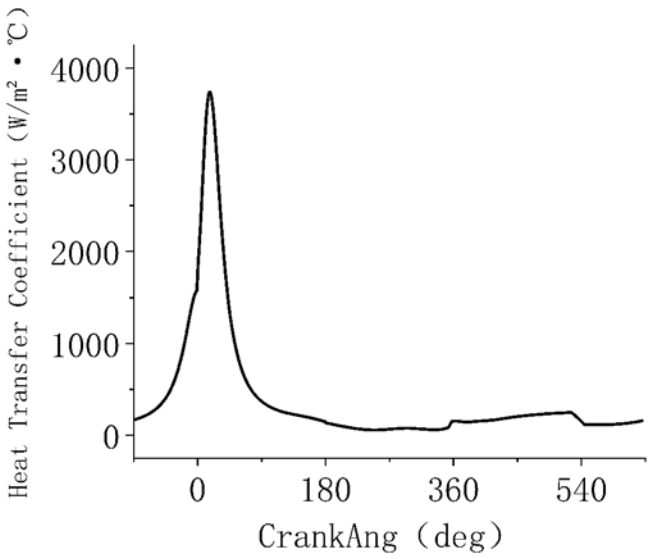

Fig. 7. Heat transfer coefficient variation curve with crankshaft rotation angle.

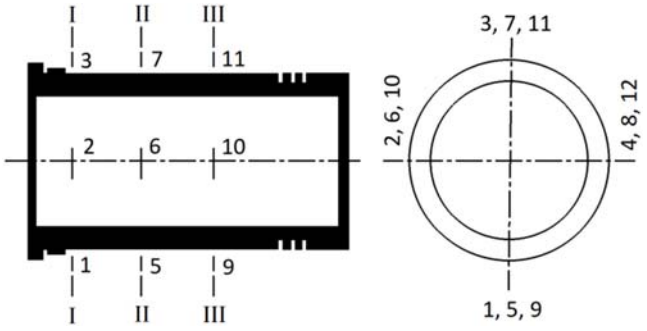

Fig. 8. Position of cylinder liner temperature measuring point.

the nodes on each path is extracted, and the final radial deformation profile of the cylinder liner is shown in Figure 9.

4 Results and discussion

4.1 Top ring surface roughness on friction performance

Taking the top ring of the piston ring as an example, the influence of piston ring surface roughness on the friction performance of the cylinder liner-piston ring friction pair is analyzed, and three different roughness of 0.8 μm, 1.2 μm and 1.6 μm are set and simulated to obtain the variation curves of asperity friction, fluid friction and total friction with engine crankshaft angle as shown in Figures 10 and 11.

As can be seen from the curves in Figure 10, the asperity friction mainly occurs near the upper dead center of the engine's work stroke. At this time, the piston ring and the cylinder liner are in the mixed lubrication state, and the friction force is generated by the micro-convex contact between the surfaces. At other times, the piston ring and cylinder liner are in a fluid lubricated state, and the asperity friction is basically zero. The change in piston ring surface roughness has a slight effect on the asperity friction, and the magnitude of its friction force increases slightly with the increase in roughness. The curves in Figure 12 show that the fluid friction force acts throughout the cycle, and the change in piston ring surface roughness has a significant effect on the fluid friction force. With the increase in piston ring surface roughness, the fluid friction decreases. This is because the increase in piston ring surface roughness facilitates the storage of lubricant on the piston ring surface and improves its frictional properties.

Figure 13 shows that the radial hydrodynamic load carrying capacity of the piston ring changes with the crank angle. It can be seen that the hydrodynamic load carrying capacity of the piston ring with a roughness of 0.8μm is significantly less than that of 1.2 μm and 1.6 μm piston rings before the stop point of the compression stroke.

The variation in the radial asperity load carrying capacity of the piston ring with the crankshaft angle is shown in Figure 14. Among them, when the roughness is 0.8 μm, the asperity load carrying capacity is slightly larger than the other two kinds of roughness, but the asperity load carrying capacity of the 1.2 μm and 1.6 μm piston rings is not much different.

Figure 15 shows the change curve of the friction loss of the top ring with the engine crankshaft angle. The friction loss of the friction pair is largest near the upper dead center of the engine work stroke, and its value increases with the increase in the roughness of the piston ring surface. At this time, the asperity friction between the piston ring and the cylinder liner plays a dominant role. The increase in roughness increases the surface area of the micro-convex body peak element contact increase, which leads to an increase in friction loss. At the other times, fluid friction plays a dominant role, the roughness of the piston ring surface is larger, and the fluid friction is smaller, so the friction loss decreases with increasing roughness.

4.2 Effect of surface roughness of piston ring set on friction performance

In addition to the top ring, the engine has two other air rings and one oil ring, and the three piston rings will also generate friction losses in operation. Figure 16 shows the four piston rings friction loss curve with the crankshaft angle change.

As seen in Figure 16, the friction loss of the top ring accounts for a higher percentage of the total friction loss compared to the other piston rings, while the oil ring friction loss accounts for the lowest percentage, and the asperity friction loss of the top ring is significantly higher than that of the other piston rings. The friction loss generated by the first three rings during the work stroke of the piston has a significant increase, and the friction loss of the oil ring does not change much in each stroke of the piston.

To study the effect of surface roughness on friction performance of different piston rings, this paper adopts the Box-Behnken experimental design method [18], in which the surface roughness of each piston ring is used as the design factor and the average friction loss is used as the response. The experimental design factors and their levels (level 0, 1, -1

Table 3. Comparison of experimental values.

	Upper temperature (K)	Middle temperature (K)	Lower temperature (K)
Calculated values	441	409	390
Experimental value	429	410	402
Error	2.79%	0.20%	2.98%

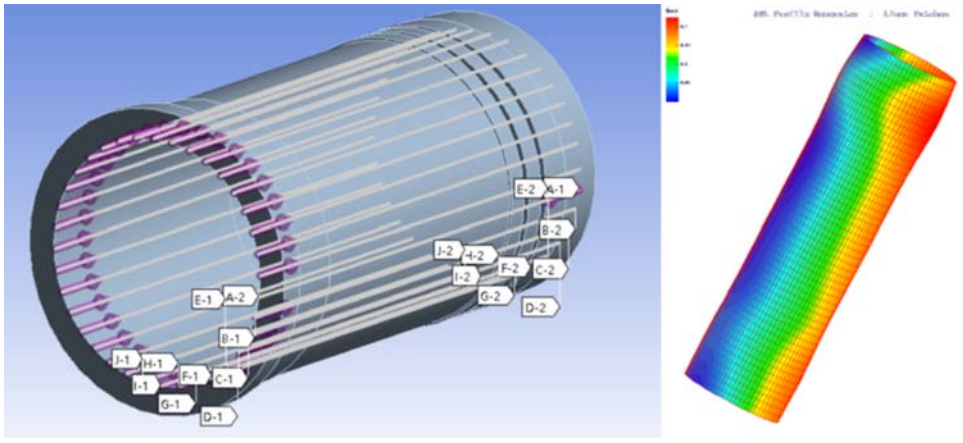

Fig. 9. Extraction of cylinder sleeve deformation profile.

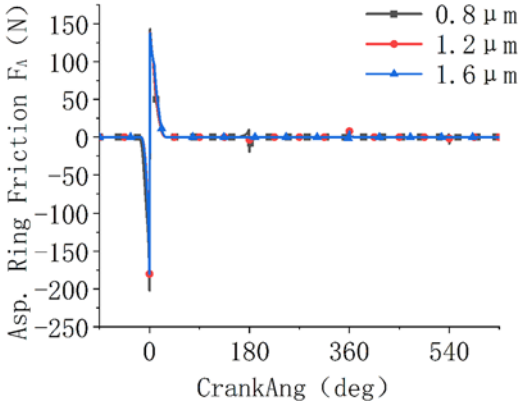

Fig. 10. Asperity friction.

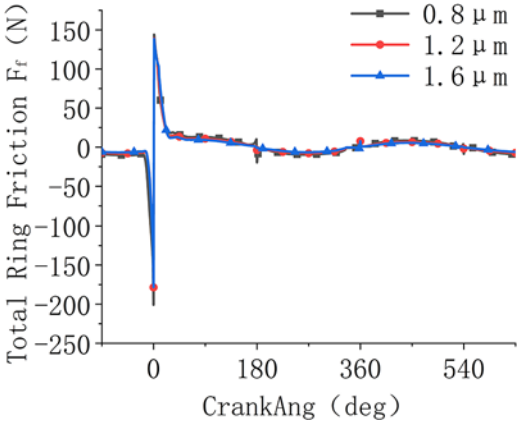

Fig. 11. Total friction.

represent three different roughness values) are shown in Table 4 [19], specific experimental arrangements are shown in Table 5, and the final combination produced 29 sets of experimental scenarios, which are shown in Figure 17.

In response surface methodology, polynomial fitting is generally used to characterize the relationship between the test factors and the response value. In this paper, based on the test grouping and its calculation results, the relationship between each factor and the response is fitted with a second-order polynomial to obtain the following regression model:

$$W = 208.01 - 12.13A - 10.48B - 13.26C - 9.10D - 0.36AB - 0.17AC - 2.67AD - 0.061BC + 0.61BD - 3.87CD + 3.60A^2 + 1.70B^2 + 3.97C^2 - 1.65D^2. \quad (20)$$

Therein: W is the average friction loss; A is the top ring roughness μm; B is the second ring roughness μm; C is the third ring roughness μm; D is the oil ring roughness μm.

Generally, to ensure the accuracy of the model, the model needs to be tested for significance. Several parameters such as the P-value of the model, the coefficient of determination R^2 and the adjusted coefficient of determination R^2_{adj} are generally used to evaluate the degree of approximation of the regression model [19]. If the P-value of the model is less than 0.05, it indicates that the model is significant. R^2 reflects the explanatory power of the regression model to the response value, the value of R^2 is generally required to be greater than 0.9. R^2_{adj} represents the correlation between all factors and the response value, the closer the value is to 1, the higher the accuracy of the

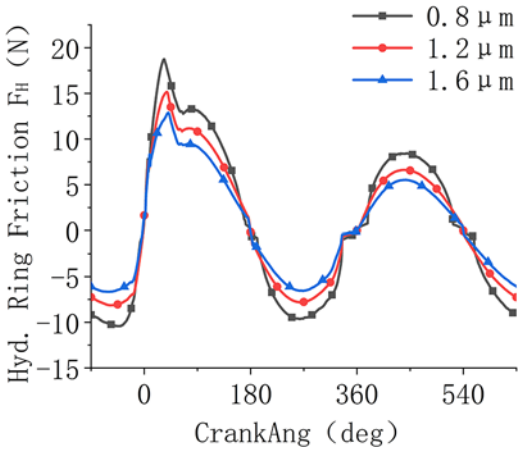

Fig. 12. Fluid friction.

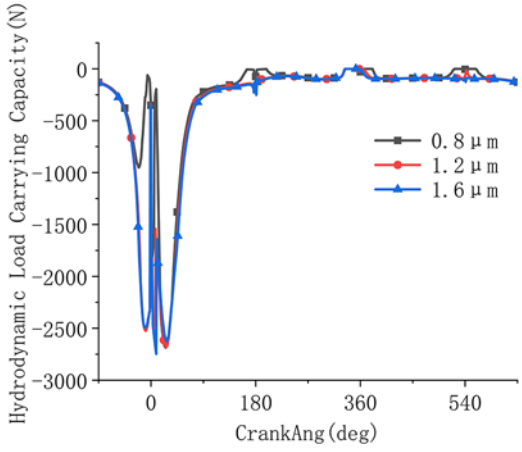

Fig. 13. Hydrodynamic load carrying capacity.

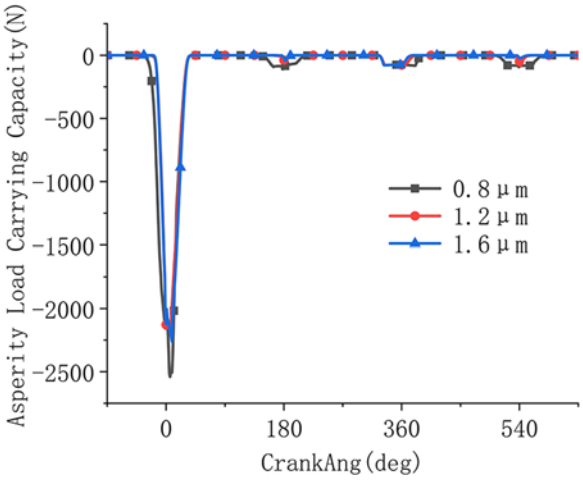

Fig. 14. Asperity load carrying capacity.

model. In this paper, the P-value of the model is less than 0.0001, that is, the model is significant. The values of R^2 and R^2_{adj} of this model are all above 0.99, which indicates that the model has high fitting accuracy and can predict the effect of piston ring surface roughness on friction performance.

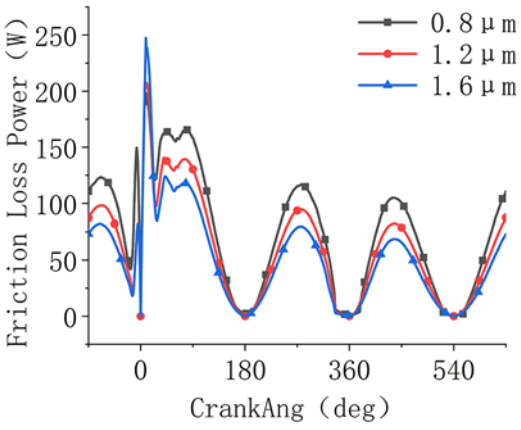

Fig. 15. Top ring roughness friction loss relationship curve.

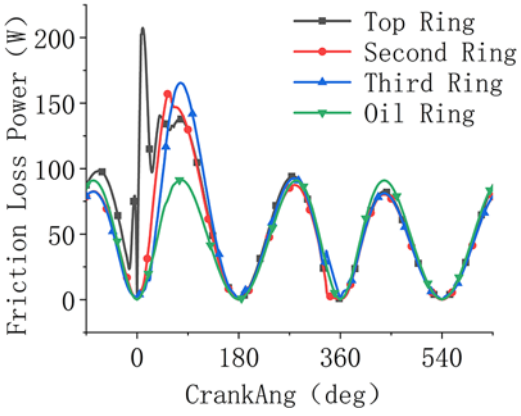

Fig. 16. Friction loss of piston ring set.

Figure 18 shows the predicted values of the regression model results compared with the original values. The information in the figure further confirms the accuracy of the model.

As seen from Figure 19, the average friction loss between the piston ring and the cylinder liner decreases with the increase in the surface roughness of each piston ring. The influence of piston ring roughness on average friction loss in the order from small to large is: oil ring, second ring, third ring and top ring. The influence of the top ring roughness is the largest, and the influence of the oil ring roughness is the smallest.

4.3 The effect of cylinder liner surface roughness on friction performance

The cylinder liner is another important part of the cylinder liner-piston ring friction pair in addition to the piston ring set, it is equally necessary to study the influence of its surface parameters on the friction performance. Three different surface roughness of the cylinder liner are selected for calculation and comparison, the surface roughness of the cylinder liner is 0.8 μm, 1.2 μm and 1.6 μm, and the surface roughness of each piston ring is 0.8μm. When the surface roughness is 0.8 μm, the total friction force and friction loss are minimal. When the surface roughness of the

Table 4. Box-Behnken design factors and levels.

level	Top ring roughness(μm)	Second ring roughness(μm)	Three ring roughness(μm)	Oil ring roughness(μm)
–1	0.8	0.8	0.8	0.8
0	1.2	1.2	1.2	1.2
1	1.6	1.6	1.6	1.6

Table 5. Experimental design of Box-Behnken design.

No.	Top ring roughness(μm)	Second ring roughness(μm)	Three ring roughness(μm)	Oil ring roughness(μm)
1	1.6	0.8	1.2	1.2
2	1.2	0.8	1.2	1.6
3	1.2	1.2	1.2	1.2
4	0.8	0.8	1.2	1.2
5	0.8	1.6	1.2	1.2
6	1.2	1.2	0.8	0.8
7	1.6	1.6	1.2	1.2
8	1.2	0.8	0.8	1.2
9	1.6	1.2	0.8	1.2
10	1.6	1.2	1.2	1.6
11	1.2	1.6	1.2	1.6
12	1.2	1.2	1.2	1.2
13	0.8	1.2	1.6	1.2
14	1.2	0.8	1.2	0.8
15	0.8	1.2	0.8	1.2
16	0.8	1.2	1.2	1.6
17	0.8	1.2	1.2	0.8
18	1.6	1.2	1.2	0.8
19	1.2	1.2	1.2	1.2
20	1.2	0.8	1.6	1.2
21	1.2	1.6	1.2	0.8
22	1.2	1.2	0.8	1.6
23	1.2	1.2	1.2	1.2
24	1.2	1.6	1.6	1.2
25	1.2	1.2	1.6	0.8
26	1.6	1.2	1.6	1.2
27	1.2	1.6	0.8	1.2
28	1.2	1.2	1.2	1.2
29	1.2	1.2	1.6	1.6

cylinder liner increases, the friction force of the micro-convex body near the upper dead center of the work stroke is slightly reduced, but the fluid friction force and friction loss increase with the increase in the surface roughness of the cylinder liner. The total friction force and friction loss of the cylinder liner-piston ring friction pair with the crankshaft angle for three different roughness are shown in Figure 20 and 21.

5 Conclusion

This paper briefly describes the theoretical model of the piston ring cylinder liner friction pair, and establishes the engine thermodynamic model and the piston ring group dynamics model to calculate the friction performance between the piston ring and the cylinder liner. The influence of surface roughness of piston ring and cylinder liner on friction

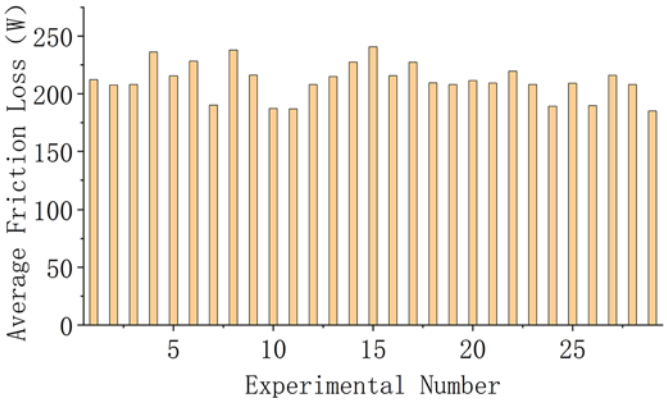

Fig. 17. Experimental scheme and calculation results.

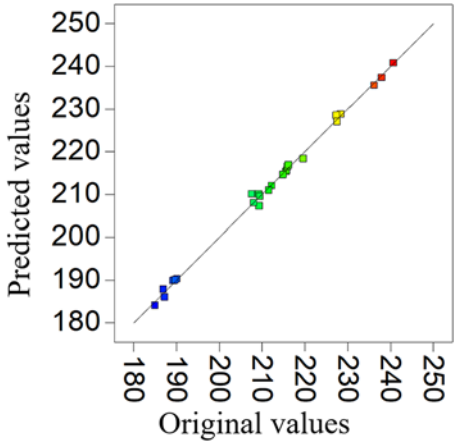

Fig. 18. Comparison of predicted and original calculated value.

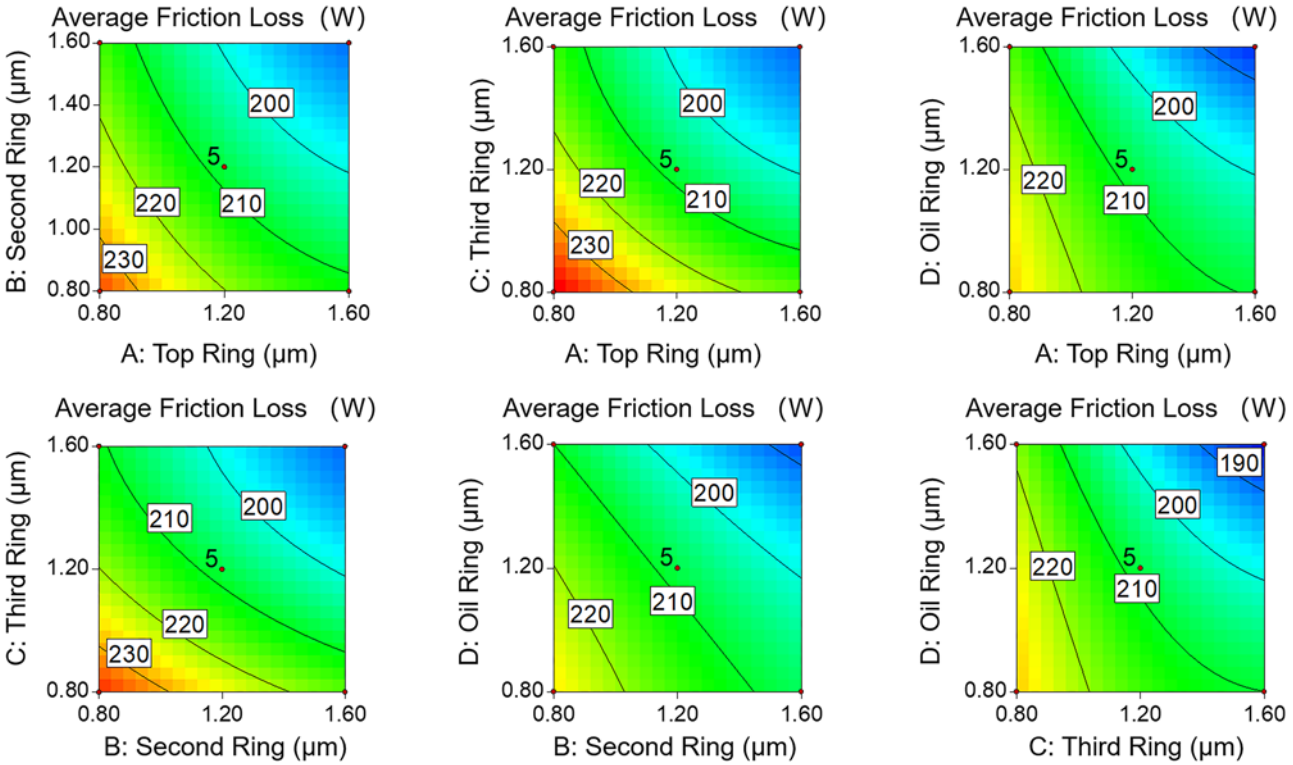

Fig. 19. Effect of surface roughness of individual piston rings on the average friction loss.

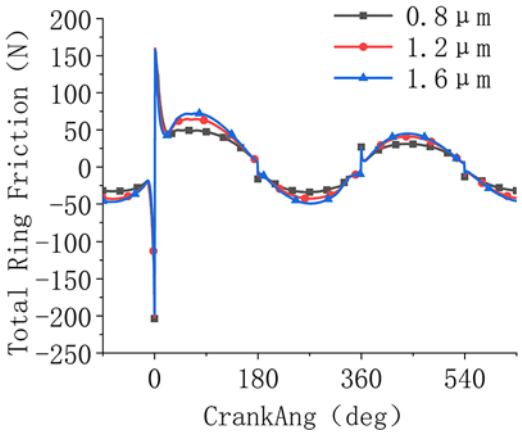

Fig. 20. Cylinder liner roughness friction relationship curve.

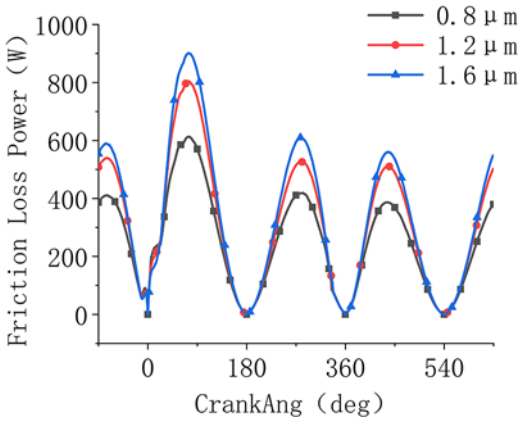

Fig. 21. Cylinder liner roughness friction loss relationship curve.

performance was analyzed. Taking into account the coupling effect of multiple piston rings, the influence of roughness variation of four piston rings on friction loss in the piston ring group is calculated by response surface methodology, and the following conclusions are obtained:

- The top ring roughness has a significant effect on the friction loss between the piston ring and the cylinder liner. With the increase in roughness, the friction loss generated by asperity friction increases, while the friction loss generated by fluid friction decreases.
- Except for the top ring, the surface roughness of other piston rings also affects the friction loss. The average friction loss between the piston ring and cylinder liner decreases with the increase in surface roughness of each piston ring. The influence of piston ring roughness changes on average friction loss in the order from small to large is: oil ring, second ring, third ring and top ring.
- The surface roughness of the cylinder liner has an equally important effect on the friction loss: as the surface roughness of the cylinder liner increases, the total friction force increases and the friction loss also increases.

Conflict of interest

The authors certify that there is no conflict of interest.

This work was supported by A Project of Shandong Province Higher Educational Science and Technology Program (No. J18KA006): Study on lubrication performance of piston ring friction pair in internal combustion engine under multi-field coupling.

List of symbols.

Variable	Definition	Unit
ϕ_x	axial pressure flow factors	dimensionless quantities
ϕ_y	circumferential pressure flow factors	dimensionless quantities
ϕ_s	hear flow factor	dimensionless quantities
ρ	lubricant density	Kg/m^3
P	oil film pressure	MPa
U	velocity of the piston ring movement	m/s
α	integrated roughness of the two surfaces of the piston ring and cylinder line	μm
σ_1	surface roughness of the piston ring	μm
σ_2	surface roughness of the cylinder liner	μm
h	nominal oil film thickness	μm
$\overline{h_t}$	expected value of the actual oil film thickness	μm
μ	lubricant dynamic viscosity	$N{\cdot}s/m^2$
p_1	the gas pressure at the upper edge of the piston ring	MPa
p_2	the gas pressure at the lower edge of the piston ring	MPa
b	the axial height of the piston ring	mm
L	the length of the piston ring in the circumferential direction	mm
W_A	the micro-convex body contact force	N
β	radius of curvature of the micro-convex body	μmm
H	film thickness ratio	dimensionless quantities
E	integrated modulus of elasticity of the two surfaces of the piston ring and the cylinder liner	MPa
E_1	the elastic modulus of cylinder liner	MPa
E_2	the elastic modulus of piston ring	MPa
υ_1	the Poisson's ratio of cylinder liner	dimensionless quantities

List of symbols. (continued).

Variable	Definition	Unit
v_2	the Poisson's ratio of piston ring	dimensionless quantities
A	nominal contact area of the micro-convex body	mm^2
A_c	actual contact area of the micro-convex body	mm^2
F_L	lubricant fluid force between the cylinder liner and piston ring	N
F_g	piston ring backlash gas force	N
F_e	piston ring own elastic force	N
P_g	the gas pressure of piston ring backlash	MPa
D	the diameter of the piston ring	mm
T	the radial thickness of the piston ring	mm
S	the opening gap of the piston ring	mm
Mg	the gravitational force of the piston ring	N
F_1	gas pressure on the lower surface of the piston ring	N
F_2	gas pressure on the upper surface of the piston ring	N
F_A	asperity friction	N
F_H	fluid friction	N
R_x	support force of the piston ring groove on the lower end surface of the piston ring	N
τ_0	the shear stress constant, the value is 2×10^6	constant
α	the boundary friction coefficient	dimensionless quantities
x_1	the starting point of the oil film	mm
x_2	the ending point of the oil film	mm
τ_1, τ_2	the shear factor	dimensionless quantities
F_f	total frictional force	N
T(s)	the cylinder liner surface temperature along with the axial height change	°C
α(s)	the heat transfer coefficient along with the axial height change	W/m^2 °C
T_m	the average temperature	°C
α_m	the average heat transfer coefficient	W/m^2 °C
k_1,k_2	$k_1=0.537(l/d)^{0.24}$, $k_2=1.45k_1$	dimensionless quantities
l	the piston stroke	mm
d	the cylinder liner inner diameter	mm
γ	$\gamma = s/l$ ($0 \leq \gamma \leq 1$)	dimensionless quantities
s	the piston axial displacement	mm

References

[1] A. Gangopadhyay, A review of automotive engine friction reduction opportunities through technologies related to tribology, Transactions of the Indian Institute of Metals **70**, 527–535 (2017)

[2] J. Sun, X. Zhang, J. Zhu et al., On the lubrication characteristics of piston ring under different engine operation conditions, Industrial Lubrication and Tribology **72**, 101–108 (2019)

[3] T. Cheng, J. Wang, S. Yao, Resecorch on Simulation and Optimization Process of a Certain Piston Ring Set Based on AVL-P&R, Diesel Engine **37**, 11–15 (2015)

[4] G. Liu, J. Sun, A Review of Research on the Lubrication of the Piston Assembly- Cylinder Friction Pair in Internal Combustion Engines, Chinese journal of automotive engineering **9**, 1–12 (2019)

[5] A. Rosenkranz, P.G. Grutzmacher, C. Gachot, H.L. Costa, Surface Texturing in Machine Elements - A Critical Discussion for Rolling and Sliding Contacts, Advanced Engineering Materials **21**, 1900194 (2019)

[6] X. Li, J. Zhao, Y. Li, G. Zhu, R. Xie, Influence of Surface Morphology of Piston Ring on Its Friction and Sealing Performances, Lubrication Engineering **46**, 70–76 (2021)

[7] H. Wu, W. Guo, S. Yin, X. Liang, Study on the Effect of Textured Inner Surface of Cylinder on the Lubrication Performance of Piston Ring, Machine Tool & Hydraulics (2020)

[8] X. Rao, C. Sheng, Z. Guo, Research on the Friction and Wear Properties of Diesel Engine Cylinder Liner with Different Surface Textures, Acta Armamentarii **39**, 356–363 (2018)

[9] X.R. Liu, G.X. Li, S.Z. Bai, Y.P. Hu, Mixed Lubrication and Friction Power Loss of Piston Ring Pack, Applied Mechanics and Materials. Trans Tech Publ, 2014, pp. 205–208

[10] N. Patir, H. Cheng, An average flow model for determining effects of three-dimensional roughness on partial hydrodynamic lubrication (1978)

[11] J. Fei, H. Luo, B. Zuo, Z. Wei, Y. Yang, H. Xu, Z. Li, An Overview of Numerical Methods for Reynolds Equation, Lubrication Engineering **45**, 130–140 (2020)

[12] J.A. Greenwood, J. Tripp, The contact of two nominally flat rough surfaces, Proceedings of the institution of mechanical engineers **185**, 625–633 (1970)

[13] X. Ye, Three-dimensional numerical simulation of piston ring lubrication and its application, Huazhong University of Science and Technology, 2004

[14] D. Wang, W. Ji, Q. Zhou, C. Zhang, Simulation of Combustion Process in Swirl Chamber of Diesel Engine,

Transactions of the chinese society for agricultural machinery. **38**, 49–52 (2007)
[15] B. Jiao, T. Li, X. Ma, C. Wang, H. Xu, X. Lu, Z. Liu, Lubrication analysis of the piston ring of a two-stroke marine diesel engine considering thermal effects, Engineering Failure Analysis **129**, 105659 (2021)
[16] H. Si, M. Li, W. Bai, C. Qi, J. Chu, Deformation analysis of the cylinder liner of a certain diesel engine in pre-tightening and working condition, Railway Locomotive and Motor Car, 14–17 (2018)
[17] X. Wang, Z. Yan, J. Zhou, Analytical and Experimental Method of Thermal Load Estimation for Diesel Engine Cylinder Liner, Chinese internal combustion engine engineering **22**, 62–65 (2001)
[18] J. Wang, L. Shen, Y. Yang, Y. Bi, M. Wan, Optimizing calibration of design points for non-road high pressure common rail diesel engine base on response surface methodology, Transactions of the Chinese Society of Agricultural Engineering 33 (2017)
[19] C. Dai, F. Kong, L. Dong, J. Wang, Y. Bai, Hydraulic and acoustic property optimization for centrifugal pump as turbine based on response surface method, Transactions of the Chinese Society of Agricultural Engineering **31**, 40–47 (2015)

Cite this article as: N. Liu, C. Wang, Q. Xia, Y. Gao, P. Liu, Simulation on the effect of cylinder liner and piston ring surface roughness on friction performance, Mechanics & Industry **23**, 8 (2022)